

# Relative densities of hydrogen ion species in a hollow cathode glow discharge

M. Fitzgerald, J. Khachan<sup>a</sup>, and S. Bosi

School of Physics, University of Sydney, 2006 Sydney, Australia

Received 17 January 2006 / Received in final form 15 February 2006

Published online 4 April 2006 – © EDP Sciences, Società Italiana di Fisica, Springer-Verlag 2006

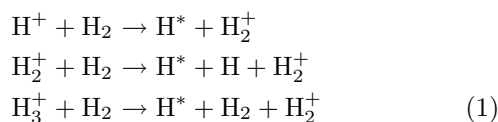
**Abstract.** Highly resolved Doppler shifted peaks of the hydrogen Balmer lines, resulting from charge exchange of  $H^+$ ,  $H_2^+$ , and  $H_3^+$  with an  $H_2$  gas target, were obtained without the need for a deconvolution procedure. This enabled the unambiguous determination of the chemistry of these hydrogen species in the units of mTorr pressure range. This was obtained from a gaseous discharge using a biconical hollow cathode that yielded a well collimated and monoenergetic beam.

**PACS.** 32.30.-r Atomic spectra – 32.30.Jc Visible and ultraviolet spectra – 32.70.-n Intensities and shapes of atomic spectral lines – 32.70.Fw Absolute and relative intensities – 32.70.Jz Line shapes, widths, and shifts – 52.70.Kz Optical (ultraviolet, visible, infrared) measurements – 52.80.-s Electric discharges

## 1 Introduction

Optical emission spectroscopy on hollow cathode hydrogen glow discharges exhibit widely broadened wings due to Doppler shift on either side of the unshifted Balmer lines [1–4]. This broadening has also been observed in plane cathode hydrogen glow discharges [5–7]. However the latter also includes backscattered ions at the cathode surface.

The origin of the shape of the broadened wings has been attributed to various mechanisms [5]. The broadened base of the central peak can be attributed to dissociative excitation of hydrogen. However, it is agreed that the energies of the atoms in the far wings result from accelerated  $H^+$ ,  $H_2^+$ , and  $H_3^+$ , which subsequently undergo charge exchange with the  $H_2$  background gas according to the following reactions [5,7]:



where  $H^*$  are energetic and excited neutrals that emit the Doppler shifted hydrogen spectrum. The relative densities of these three ionic species has not been clearly determined from past spectroscopic measurements on hollow cathode discharges.

In this paper, we present measurements that show highly resolved Doppler shifted peaks that clearly identify the three ionic species. This enabled their relative densities to be determined as a function of pressure in the units of mTorr pressure range.

To analyze the spectra, we note that it has been shown [8] that the fast neutrals,  $H^*$ , which result from charge exchange reactions, have trajectories that are in the same direction as the incident (“parent”) ions. Moreover, the total energy of the resulting fragments from the reactions is approximately equal to the energy of the incident ion. Any energy lost to electronic or vibrational excitation are only a few tens of eV and are negligible compared to the keV range of energies considered here. Note that if the parent ion is  $H_2^+$  then each of the  $H^+$  fragments will have half the energy. Similarly, for  $H_3^+$ , the fragments have a third of the parent’s energy [8].

The Doppler shift in the hydrogen  $H_\alpha$  line (656.3 nm) was used to determine the energy of the fragments, and therefore, the energy of the parent ions. However, since there are predominantly three types of charge exchange reactions as shown in equation (1) resulting in three different energies of neutral hydrogen, then one can expect three different Doppler shifted peaks of  $H_\alpha$  provided the parent ions were approximately monoenergetic. The shift in wavelength,  $\Delta\lambda$ , is given by

$$\Delta\lambda \approx \frac{v\lambda_0}{c} \cos\theta \quad (2)$$

where  $\lambda_0$  is the wavelength of the unshifted  $H_\alpha$  line (=656.3 nm),  $v$  is the speed of an excited atomic hydrogen,  $c$  is the speed of light and  $\theta$  is the angle between the observation direction and the direction of travel. Therefore, the kinetic energy,  $K$ , of an excited neutral is given by

$$K = \frac{m_H c^2 (\Delta\lambda)^2}{2\lambda_0^2 \cos^2\theta} \quad (3)$$

where  $m_H$  is the mass of atomic hydrogen.

<sup>a</sup> e-mail: j.khachan@physics.usyd.edu.au

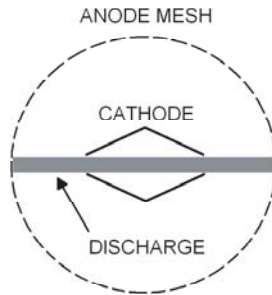


**Fig. 1.** Schematic diagram of the hollow cathode discharge set-up used, which consisted of an outer spherical (wire mesh) anode and a centered biconical cathode. A channel of discharge was generated through the cathode to the anode.

## 2 Experimental set-up

The cathode consisted of two hollow stainless steel cones attached base-to-base as shown in Figure 1. The tips of the cones were truncated to produce the two apertures which produced a single channel of discharge along the axis of the cathode. The use of this “biconical” cathode resulted in sharper and better defined spectra than previously recorded Doppler spectra on hollow cathode discharges. The circular entrance and exit of the cathode were 15 mm in diameter. The length of the cathode from entrance to exit was 55 mm. The waist of the cathode had a 30 mm diameter. The cathode was placed at the center of a spherical anode mesh, which was 200 mm in diameter.

At lower pressures,  $\sim 2$  mTorr, it was difficult to initiate the DC discharge. As a result, a hydrogen plasma generated by an RF discharge at 13.56 MHz was applied externally to the anode. This RF discharge was produced by a single loop antenna situated 40 cm below the anode and cathode assembly. The RF antenna was electrically isolated from this assembly so that no voltage bias existed between them. The power applied to the antenna was  $\sim 10$  W so that a very low density plasma drifted up towards the assembly. The spherical anode mesh consisted of 2 mm grid wire spacing and was grounded so that this acted as an RF shield as well as excluding most of the discharge generated externally. However, the small fraction of electrons that drifted through to the inside of the mesh enabled a discharge to be generated between the anode and cathode for low pressures and voltages, which would not otherwise be able to sustain the DC discharge. However, at the higher voltages and pressures the DC discharge was self-sustaining and the RF discharge made no difference to the spectroscopy presented here. Moreover, the recorded hydrogen spectrum within the anode was at noise level whenever the DC discharge was switched off and the RF discharge remained on, so that we can be certain that the RF discharge made almost no contribution to the spectroscopy. However, for consistency, the RF discharge was kept on throughout the series of measurements presented here.

The DC discharge appeared as a linear beam along the axis of the cathode with the maximum emission intensity at the cathode center. There was a faint discharge arising

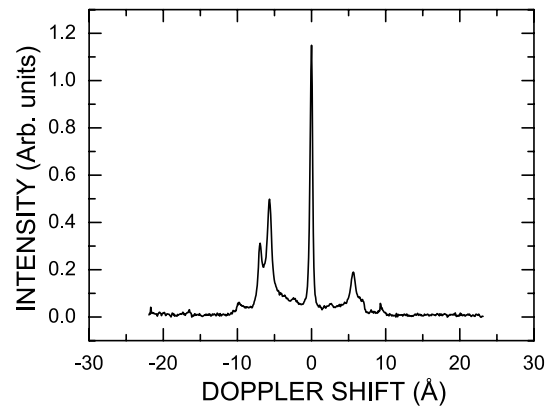


**Fig. 2.** Doppler shifted hydrogen spectrum of the  $H_{\alpha}$  Balmer line viewed along the axis for the hollow cathode operating at a voltage of  $-4.5$  kV and a pressure of 5 mTorr.

from the ions that strike the outer surface of the cathode. However, these did not contribute to our spectroscopic measurements since the objective lens of the monochromator was focussed on the inside center of the cathode. The anode was held at the same potential as the vacuum chamber containing the plasma. The plasma on the outside of the anode was kept at very low densities and the anode grid mesh spacing was of the order of a Debye length, which greatly reduced the density of the plasma that penetrated through the mesh, but still permitted a trickle of ions and electrons to ensure that the discharge within the anode was self-sustaining. Therefore pressure and voltage could be varied independently without extinguishing the discharge. The anode also acted as a radio-frequency radiation shield to ensure that the discharge was purely DC. The current collected by the cathode was  $\sim 1$  mA.

The hydrogen Balmer  $H_{\alpha}$  line (656.3 nm) was detected with an intensified charge-coupled device (Princeton Instruments ICCD 576G/RB-E) mounted on a 0.5 m focal length monochromator (Spex 500M). The wavelength resolution of the set-up was 0.04 nm. The line of sight of the monochromator was coincident with the axis of the cathode.

## 3 Results and discussion

A sample of a Doppler-shifted spectrum is shown in Figure 2. This spectrum consists of the central unshifted  $H_{\alpha}$  transition arising from excited low energy neutral hydrogen. The peaks on either side of the central peak are the red and blue shifted peaks of excited neutrals,  $H^*$ , resulting from the charge exchange processes given in equation (1). Although this spectrum is symmetrical in wavelength shift, the heights of the peaks are not equal. The intensity of the blue shifted peaks is greater than that of the red shift. The reason for this is non-trivial and will be the subject of a future publication. Otherwise, the spectrum is completely symmetric along the horizontal axis. That is, the ions travelling towards and away from the

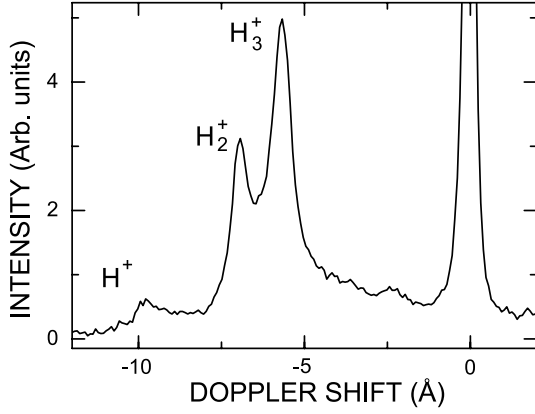


**Fig. 3.** The blue shifted  $H_\alpha$  spectrum obtained from the biconical cathode with a  $-4.5$  kV cathode voltage and a pressure of 5 mTorr. The labels  $H^+$ ,  $H_2^+$ , and  $H_3^+$  on the three prominent peaks indicate the parent ion that gave rise to the peak from energetic atomic hydrogen, which results from charge exchange reactions with the background hydrogen gas.

center have equal energies as would be expected. However, of interest to us is the detail in the Doppler shifted peaks.

These Doppler peaks are unusually sharp because the parent ions that give rise to the observed energetic neutrals are very nearly monoenergetic, and the design of the cathode ensures that the parent ion (and hence neutral) motions are well-collimated. Consequently, this enabled the reliable study of the chemistry under different pressures.

Figure 3 is an enlargement of the blue shifted spectrum. We selected this peak for analysis because it was the more intense of the two. Note that this peak consists of three distinct peaks that we have labelled as  $H^+$ ,  $H_2^+$ , and  $H_3^+$ . The labels indicate the parent ion that gave rise to the energetic neutral responsible for a peak. Although these are all energetic excited neutral hydrogen, there are clearly three distinct energies corresponding to the three charge exchange processes given in equation (1). Using equation (3), the energies of the three peaks were determined for cathode voltages ranging from  $-2.5$  to  $-9.5$  kV, as shown in Figure 4. Note that in the cases of incident  $H_2^+$  and  $H_3^+$  the energy of the resulting  $H^*$  must be doubled and tripled, respectively, since energy is equipartitioned between the individual H atoms of the parent ion. In each case it was found that the energy of the three incident ionic species increases linearly by  $0.3$  keV per  $1$  kV increase in cathode potential. In Figure 4 each plot symbol actually represents three concentric data points, one for each of the charge exchange reactions arising from the three types of parent ions ( $H^+$ ,  $H_2^+$ , and  $H_3^+$ ), the scatter being smaller than the size of the plot symbol. It was not possible to resolve the peaks below  $1$  kV cathode voltage, however it is unlikely that the curve is linear below this region since momentum transfer collisions start to dominate. The energies obtained can now be used with intensity measurements in order to determine the relative ion densities.

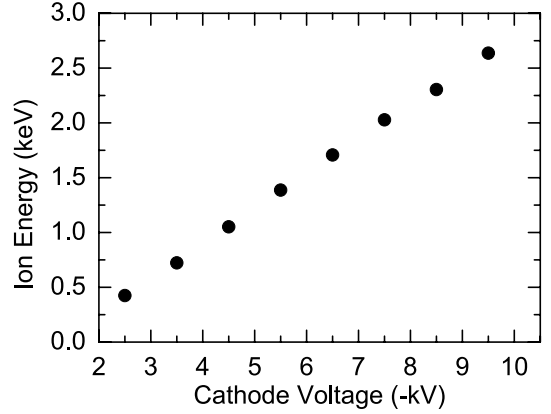


**Fig. 4.** Ion energies of  $H^+$ ,  $H_2^+$ , and  $H_3^+$  as a function of applied cathode voltage. All three plots fall precisely on the same points within the resolution of the graph indicating that all three parent ions had the same energy.

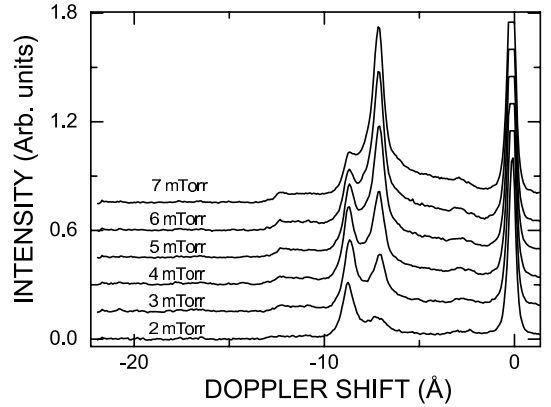
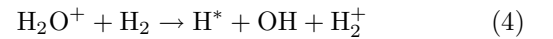


**Fig. 5.** Relative intensity variation with increasing pressure. Six different spectra are superimposed and shifted upwards with increasing pressure from 2 mTorr to 7 mTorr. Cathode bias with respect to the grounded anode was kept at  $-6$  kV.

Note also from Figure 3 that there is a small peak at a shift of  $-2.5$  Å. This corresponds to charge exchange of an ion of atomic mass unit of 18 with the background gas resulting in energetic atomic hydrogen. This suggests that it is probably a water molecule ion taking part in the following charge exchange reaction



where emission from the excited hydrogen,  $H^*$ , is the above mentioned peak that is being detected. We mention the origins of this peak for completeness but is of no further interest in this paper.

### 3.1 Ionic species' density

Figure 5 shows spectra obtained for six different pressures, successive graphs being translated vertically to aid visibility. Using the positions and relative intensities of the three prominent peaks we obtained the energies and relative densities of the different parent ions ( $H^+$ ,  $H_2^+$ ,  $H_3^+$ ), respectively.

It is clear from Figure 5 that the relative intensities of the different species change with pressure, as is particularly evident in the increasing relative intensity of the  $H_3^+$  peak. As a result, it is possible to determine the relative densities of the three ionic species. The total intensity,  $I_n(H_x^+)$ , from the  $H_\alpha$  line due to charge-exchange between  $H_x^+$  (where  $x = 1, 2, \text{ and } 3$ ) and the background gas is directly proportional to the power emitted per unit volume given by

$$I_n(H_x^+) \propto h\nu A_{3 \rightarrow 2} n_{H^*}(H_x^+) \quad (5)$$

where  $h$  is Planck's constant,  $\nu$  is the frequency of the emitted photons,  $A_{3 \rightarrow 2}$  is the transition probability between the  $n = 3$  and  $n = 2$  energy levels of atomic hydrogen, and  $n_{H^*}(H_x^+)$  is the number density of the atomic hydrogen in the  $n = 3$  state that results from a charge-exchange reaction between  $H_x^+$  and the background gas. We can obtain  $n_{H^*}(H_x^+)$  by considering its rate of change given by

$$\frac{dn_{H^*}(H_x^+)}{dt} = n_{H_x^+} n_{H_2} k_{H_x^+} - \sum_{i=1}^2 A_{3 \rightarrow i} n_{H^*}(H_x^+) - k_q n_{H_2} n_{H^*}(H_x^+) \quad (6)$$

where  $n_{H_x^+}$  is the number density of incident  $H_x^+$ ,  $n_{H_2}$  is the number density of the  $H_2$  background gas,  $k_{H_x^+}$  is the charge-exchange rate coefficient resulting in excited atomic hydrogen,  $A_{3 \rightarrow i}$  is the transition probability between the  $n = 3$  and  $n = i$  energy levels of excited atomic hydrogen (where  $i = 1, 2$ ), and  $k_q$  is the quenching rate coefficient. We will only consider quenching due to the background gas,  $H_2$ , since its density is much greater than any other species present.

Equation (6) balances the rate of production and loss of atomic hydrogen in the  $n = 3$  energy level. The first term on the right hand side is the rate at which excited atomic hydrogen is created from charge-exchange collisions. The second term is the rate of de-excitation from the same state due to spontaneous emission. The third term represents de-excitation from  $n = 3$  due to radiationless transitions from collisions with  $H_2$  (quenching).

For a continuous discharge, we can apply the steady state condition  $dn_{H^*}(H_x^+)/dt = 0$ , which simplifies equation (6) to

$$n_{H_x^+} = \frac{(\sum_{i=1}^2 A_{3 \rightarrow i} + k_q n_{H_2}) n_{H^*}(H_x^+)}{n_{H_2} k_{H_x^+}}. \quad (7)$$

We can assume that the quenching rate coefficient is the same for all three energy peaks since the quenching cross-section would not change significantly at these high energies. Using equation (5), we can obtain the relative number densities of  $H_3^+$  and  $H_2^+$  with respect to the density of  $H^+$  given by

$$\frac{n_{H_x^+}}{n_{H^+}} = \frac{k_{H^+} I_n(H_x^+)}{k_{H_x^+} I_n(H^+)}. \quad (8)$$

The intensities  $I_n(H_x^+)$  were obtained from the area under the Gaussian fits of the three peaks. The charge-exchange

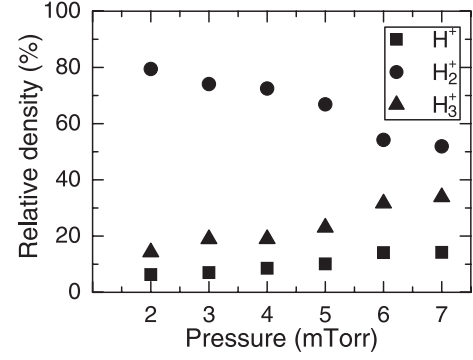


**Fig. 6.** Relative ion density variation with increasing pressure for  $H^+$ ,  $H_2^+$ , and  $H_3^+$  for the discharge at  $-6$  kV.

rate coefficients,  $k_{H_x^+}$ , are given by

$$k_{H_x^+} = \int \sigma_{H_x^+} v f(v) dv \quad (9)$$

where  $\sigma_{H_x^+}$  is the charge-exchange cross-section leading to an excited hydrogen neutral above the  $n = 2$  energy level,  $v$  is the velocity of the incident ion, and  $f(v)$  is the velocity distribution function. The directional peaks in the spectrum were treated as monoenergetic to a first order approximation since their widths approached the resolution of the monochromator. Consequently, the rate coefficient now simplifies to

$$k_{H_x^+} = \sigma_{H_x^+} v_{H_x^+} \quad (10)$$

where  $v_{H_x^+}$  is the velocity of the  $H_x^+$  ions obtained from the center of the Doppler shifted peaks. The density ratio now becomes

$$\frac{n_{H_x^+}}{n_{H^+}} = \frac{\sigma_{H^+} \Delta\lambda_{H^+} I_n(H_x^+)}{\sigma_{H_x^+} \Delta\lambda_{H_x^+} I_n(H^+)} \quad (11)$$

where  $\Delta\lambda_{H_x^+}$  is the Doppler shift of the peak associated with the  $H_x^+$  incident ion. The charge-exchange cross-sections for atomic hydrogen excitation were obtained from Phelps [9]. These were  $0.033 \times 10^{-20} \text{ m}^2$ ,  $0.016 \times 10^{-20} \text{ m}^2$ , and  $0.056 \times 10^{-20} \text{ m}^2$  for the energies of  $H^+$ ,  $H_2^+$ , and  $H_3^+$ , respectively.

Figure 6 shows a plot of relative ion densities in the discharge. The error in the relative densities, which depends on the peak widths in the spectrum, is covered by the size of the plot symbols. The relative densities of the three ion species have been normalized so that their sum is 100%. This shows there is a significant increase in the relative  $H_2^+$  density with a reduction in pressure. In particular, relative to the sum of densities of the three hydrogen ions, the relative density of  $H_3^+$  doubles with a pressure increase of only 5 mTorr, whereas the relative density of  $H_2^+$  almost halves.

## 4 Conclusion

We have presented highly resolved Doppler shift spectra that clearly show the three dominant ionic species present

in a hydrogen hollow cathode discharge. Using the relative intensities of excited atomic hydrogen, which results from charge exchange of these ions with the background gas, and a simple steady state collisional radiative model, we have determined the relative hydrogen ion densities as a function of pressure. It was shown that as pressure in the units of mTorr pressure regime was increased, the relative density of  $H_2^+$  ions decreased relative to the density of  $H_3^+$  ions, with a minor component being the  $H^+$  density.

It is tempting to extend the use of this technique to RF processing hydrogen plasmas since in principle the same analysis can be carried out provided the RF electric field is linear. There has been work on RF discharges [10] that has shown structure in the Doppler shifted hydrogen Balmer lines. But in reality for higher pressure, of the order 100 mTorr, it will not be possible due to considerable broadening of the Doppler shifted peaks, which makes them indistinguishable from each other.

## References

1. W. Benesch, E. Li, *Opt. Lett.* **9**, 338 (1984)
2. E. Ayers, W. Benesch, *Phys. Rev. A* **37**, 194 (1988)
3. N.M. Šišović, G. Lj. Majstorović, N. Konjević, *Eur. Phys. J. D* **32**, 347 (2005)
4. N. Konjević, G. Lj. Majstorović, N.M. Šišović, *Appl. Phys. Lett.* **86**, 251502 (2005)
5. C. Barbeau, J. Jolly, *J. Phys. D: Appl. Phys.* **23**, 1168 (1990)
6. M. Kuraica, N. Konjević, *Phys. Rev. A* **46**, 4429 (1992)
7. M.R. Gemišić Adamov, B.M. Obradović, M.M. Kuraica, N. Konjević, *IEEE Trans. Plasma Sci.* **31**, 444 (2003)
8. G.W. McClure, *Phys. Rev.* **140**, A769 (1965)
9. A.V. Phelps, *J. Phys. Chem. Ref. Data* **19**, 653 (1990)
10. G. Baravian, Y. Chouan, A. Ricard, G. Sultan, *J. Appl. Phys.* **61**, 5249 (1987)